Nucl. Sci. and Tech., Vol.6, No. 3 (2016), pp. 60-66

Nuclear Science and Technology

Journal homepage: https://jnst.vn/index.php/nst

# The efficient neutron-gamma pulse shape discrimination with small active volume scintillation detector

Phan Van Chuan[1], Nguyen Duc Hoa[1], Nguyen Xuan Hai[2], Nguyen Ngoc Anh[2], Tuong Thi Thu Huong[2], Nguyen Nhi Dien[2], Pham Dinh Khang[3]

[1]*Dalat University, 01 Phu Dong Thien Vuong, Dalat, Lam Dong, Vietnam*
[2]*Nuclear Research Institute, 01 Nguyen Tu Luc, Dalat, Lam Dong, Vietnam*
[3]*Hanoi University of Science and Technology, 01 Dai Co Viet, Hanoi, Vietnam*

**Abstract:** A small detector with EJ-301 liquid scintillation was manufactured for the study on the neutron-gamma pulse shape discrimination. In this research, four algorithms, including Threshold crossing time (TCT), Pulse gradient analysis (PGA), Charge comparison method (CCM), and Correlation pattern recognition (CPR) were developed and compared in terms of their discrimination effectiveness between neutrons and gamma rays. The figures of merits (FOMs) obtained for 100 ÷ 2000 keVee (*keV energy electron equivalent*) neutron energy range show the charge comparison method was the most efficient of the four algorithms.

**Keywords:** *EJ-301 liquid scintillation detector, threshold crossing time, pulse gradient analysis, charge comparison, correlation pattern recognition.*

## I. INTRODUCTION

The neutron - gamma (n-γ) pulse shape discrimination (PSD) techniques are very important in the fast neutron measurement using the scintillation detectors. Among of these detectors, the EJ-301 liquid scintillation detector has been widely employed because of their excellent neutron-gamma discrimination, high efficiency for the fast neutron detection and superior time resolution. It detects both neutron and gamma ray and the two particle types can be distinguished by analyzing the shapes of measured pulses.

Various n-γ PSD techniques have been developed, including both analog and digital approaches such as zero-crossing method, constant fraction discriminator [1,2], charge comparison [2,3], frequency gradient analysis [4], threshold crossing time, correlation pattern recognition methods [5], etc.

Fast electronics development has created new techniques such as flash analog digital convertor (ADC), field programmable gate array (FPGA), and digital signal processing (DSP). That makes the PSD methods widely applied. In modern PSD systems, pulses from detector are digitized by flash ADC and the data are stored in memory and analyzed by PSD method on computer[5-7], or on the board FPGA/DSP [4]. Almost studies of neutron - gamma PSD were performed on different detectors; however, the evaluation of neutron-gamma PSDs' capacities has not been carried out. In this work, a prototype of a small active volume scintillation detector was made for studying neutron and gamma measurement. Based on the digitized pulses from the detector, the four algorithms of RTD, PGA, CCM and CPR have been used to evaluate the detector's efficiency for neutron-gamma discrimination.

https://doi.org/10.53747/jnst.v6i3.169
Received 13 September 2016, accepted 07 December 2016

## II. EXPERIMENT

### A. Experiment setup

The prototype detector's intrinsic volume has the dimensions of 34mm in diameter and 60mm in length. It was filled with EJ301 liquid scintillator and encapsulated in an aluminum cell whose walls were1mmthick and well-polished. The scheme of the detector is shown in Fig. 1. The scintillation cell was contacted with a Hamamatsu R9420 photomultiplier tube (PMT) with operating negative voltage of 1200V through a 2 mm thick ultra violet glass layer. The output pulses from the anode of the PMT which had very short rise time (less than 5ns) and small amplitude were not digitized convenient. Because of that, a fast preamplifier was connected directly to the anode of the PMT. The preamplifier would shape the pulses which had the rise time of approximately 10ns and fall time of approximately 30ns. These shapes removed the causes of distortion in cables, but retained the different characteristics of scintillator pulses induced by neutron or gamma particles. Because slower decay time-constant of EJ301 is about 32ns, the characterized difference between neutron and gamma would be located in the tail of the pulse.

The detector testing was done with radioactive sources and digital oscilloscope. Fig. 2 shows the layout of experimental arrangement; in which the high voltage power supply was a model 3002D and detector's output was connected to the input of oscilloscope model DPO7254C. The standard gamma ray sources ($^{22}$Na, $^{60}$Co and $^{137}$Cs) were also used to initially characterize the energy performance of the detector. The $^{252}$Cf neutron source with the activity of approximately 3.0 mCi was used to evaluate the detector's efficiency of neutron-gamma separation. The DPO7254C with 8-bit resolution was operated on sampling rate of 1 Giga-sample per second. The sampling data were saved on a memory stick for off-line analysis.

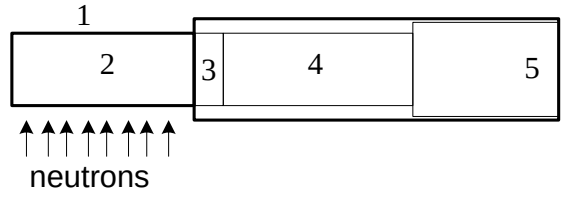


**Fig. 1.** Scheme of neutron detector: (1) detector vessel; (2) liquid scintillator; (3) UV window glass; (4) PMT; (5) Preamplifier (Preamp).

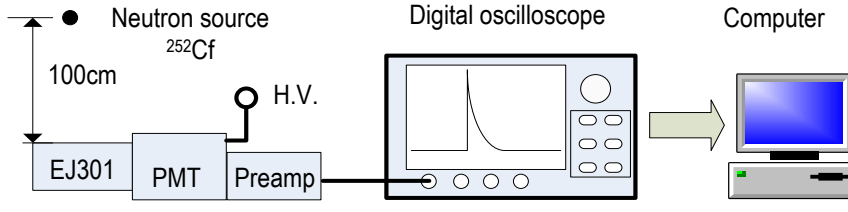


**Fig. 2.** Diagram of the experimental setup.

### B. Data analysis

The typical pulse shapes of the EJ-301 liquid scintillation detector are shown in Fig. 3; the neutron pulses exhibit a larger decay time to the base line, which is due to a greater proportion of the slow scintillation component. The PSD methods are based on the different characteristics in the pulse tails of neutrons and gamma-rays. In this work, TCT, PGA, CCM and CPR methods were applied for data analysis.

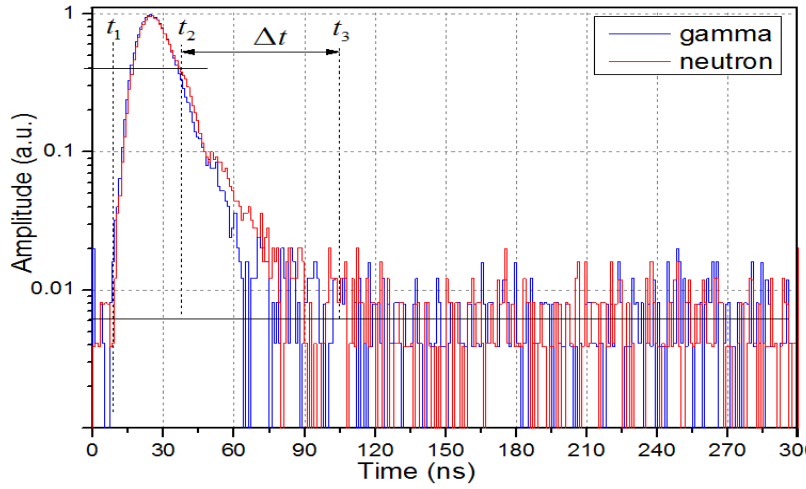


**Fig. 3.** Typical sample of detector signals for neutron and gamma ray in one sampling frame.

a) TCT method is carried out by measuring the time interval (Δt) between the time where the pulse amplitude begins to fall ($t_2$) and the time where the amplitude cuts the threshold ($t_3$) (see Fig. 3). The time where the amplitude is over the threshold of neutron pulses is greater than that of the gamma pulses, so it was used as a parameter to neutron - gamma PSD.

b) PGA method is gradient analysis of the integrated pulses to discriminate neutron and gamma radiation. The value of gradient is based on the comparison of the relative heights of the samples at the pulse tail, and determined by equation (1) [11].

$$\delta = \left|\frac{dV(t)}{dt}\right| = \left|\frac{V(k+nT) - V(k)}{nT}\right| \quad (1)$$

Where *V(k)* is the amplitude of the $k^{th}$ in sampling period *T* and *n* is the number of sampling periods. In approximation, if *n* is a constant, then $\delta \approx |V(k+nT) - V(k)|$.

c) CCM is based on area comparison of the rising or the falling portions of a pulse. Because the pulse gradient of neutrons is different from that of gamma rays; therefore, the ratios of a pulse area are also changed. The area S of the pulse was calculated based on equation (2) [5].

$$S = \int_{t_1}^{t_2} V(t)dt = \sum_{k=1}^{n} V(k).\Delta t \quad (2)$$

Where *V(k)* is the amplitude of the $k^{th}$ in sampling period *T*, $t_1$ and $t_2$ are timing of beginning and ending of sampling period and Δt = $t_2 - t_1$.

d) For CPR method, a signal is considered as an object vector X whose components are the digitized amplitude $x_n$ of the signal at sampling time $t_n$. CPR is performed by taking a scalar product of this vector with the reference vector Y which describes a gamma ray or neutron signal [5].

$$\vec{X} = (x_1, x_2, ..., x_n); \qquad \vec{Y} = (y_1, y_2, ..., y_n) \quad (3)$$

$$r = \frac{\vec{X}.\vec{Y}}{\left|\vec{X}\right|.\left|\vec{Y}\right|} \quad (4)$$

Where, *r* is the correlation coefficient between vector $\vec{X}$ and vector $\vec{Y}$, $\vec{X}.\vec{Y}$ is scalar product, $|X|$ and $|Y|$ are the norm of the vectors X and Y respectively.

$$\theta = Acr\cos\frac{\sum_{i=1}^{n} x_i.y_i}{\sqrt{\sum_{i=1}^{n} x_i^2}\sqrt{\sum_{i=1}^{n} y_i^2}} \quad (5)$$

Where, $\theta(rad)$ is the angle between the vectors; the $\theta$ value indicates the similarity of the object vector with the reference vector.

### C. Evaluation of pulse shape discrimination

The FOM was used to evaluate the quantitative results of neutron-gamma discrimination, and defined by equation 6.

$$FOM = \frac{Ch_n - Ch_\gamma}{FWHM_n + FWHM_\gamma} \quad (6)$$

Where, $Ch_n, Ch_\gamma$ are the positions of neutron and gamma peaks respectively; $FWHM_n$ and $FWHM_\gamma$ are the full-width-half-maximums of neutron and gamma peaks respectively, in the histogram.

## III. RESULTS AND DISCUSSION

### A. Results

Fig. 4 shows the amplitude spectra which were measured with radioisotope sources of $^{60}$Co, $^{22}$Na and $^{137}$Cs. The upper inset plot shows the results of amplitude calibration in which its points are the positions of Compton edges coinciding with the gamma peaks induced from radioisotope sources. These data points were fitted with a linear model with first order function as E(Ch) = 0.188×Ch - 30.55; where E and Ch are energy and channel, respectively.

The measured data with a neutron source $^{252}$Cf were analyzed by the methods of TCT, PGA, CCM and CPR. The scatter plots of the n-γ separation with energy threshold of 100keVee by four methods are shown in Fig. 5, 6, 7 and 8.

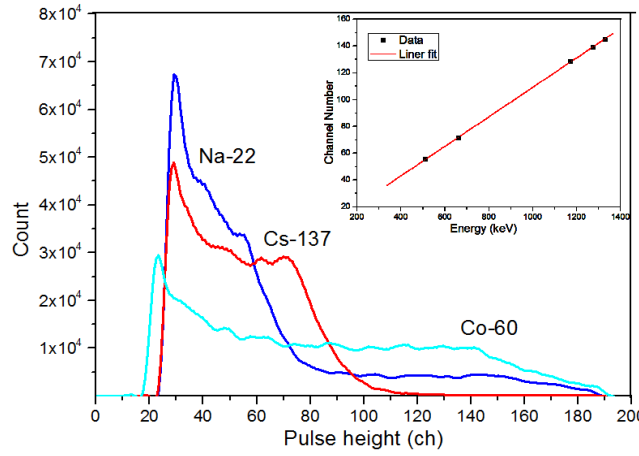


**Fig. 4.** Pulse height distribution from sources of $^{60}$Co, $^{22}$Na and $^{137}$Cs. The upper inset shows the calibration data using the Compton edges of the gamma - ray *spectra*

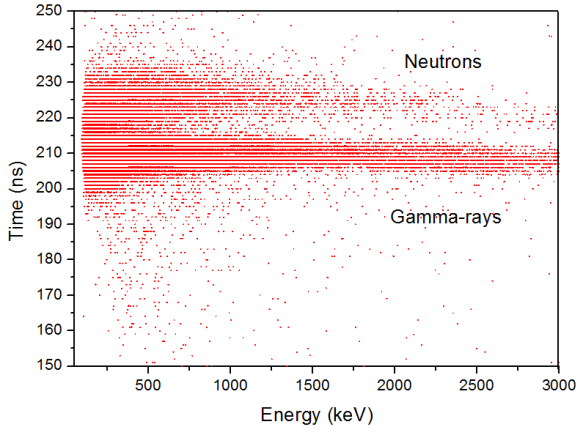


**Fig. 5.** Threshold crossing time versus pulses

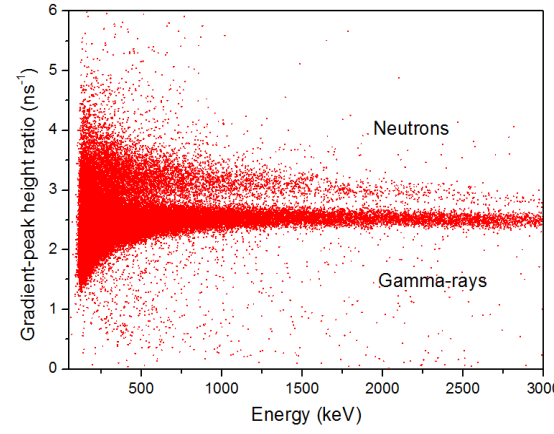


**Fig. 6.** Pulses gradient versus pulse height

Fig. 5 shows the two-dimensional plot of threshold crossing time versus pulse amplitude. The data in Fig. 5 show that n-γ PSD of the pulse heights for each waveform in the energy region greater than 500 keVee is good. Fig.6 is the scatter plot of gradients versus pulse heights for each waveform. Fig.7 shows the scatter plot of area ratios of pulse tails versus pulse heights for each waveform. Fig.8 is the scatter plot of angle ratios versus pulse heights for each waveform. Based on the analytical results, the discrimination between neutron-gamma pulses in the RTD and CCM methods are better than the PGA and CPR methods in the high energy region (> 200 keV).

Fig. 9, 10, 11 and 12 are the statistical charts of four methods, the energy threshold was set at 800keV.

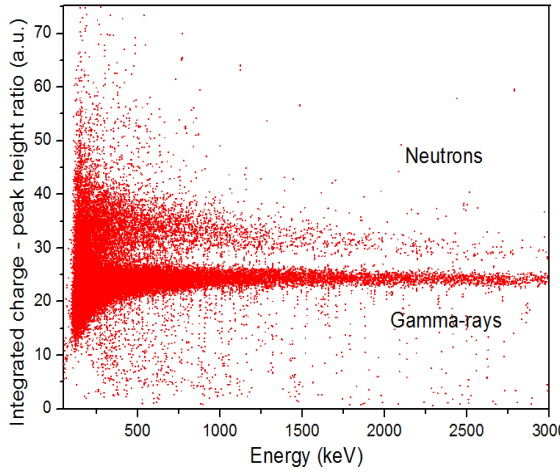


**Fig. 7.**The integrated charge versus pulse heights

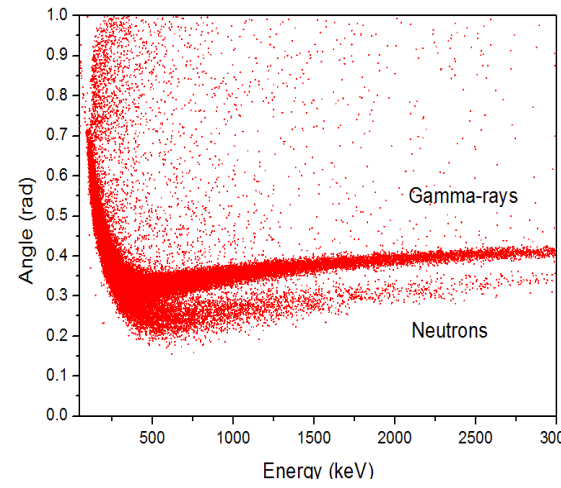


**Fig. 8.** Angle ratios versus pulse heights

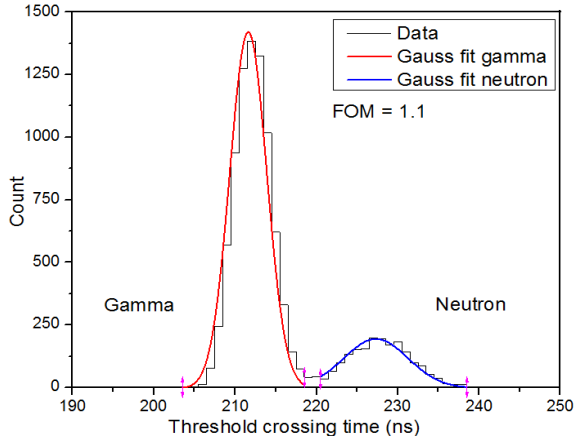


**Fig. 9.** Histogram of threshold crossing time

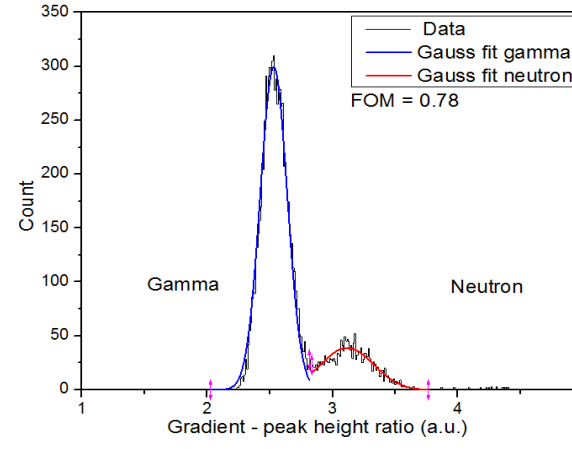


**Fig. 10.** Histogram of pulse gradient analysis

Fig. 12 shows the distribution of FOM values of methods as threshold crossing time, pulse gradient analysis, charge comparison, and correlation pattern recognition in the range of energy from 100 to 2000keVee.

Fig. 12 shows the distribution of FOM values of methods as threshold crossing time, pulse gradient analysis, charge comparison, and correlation pattern recognition in the range of energy from 100 to 2000keVee.

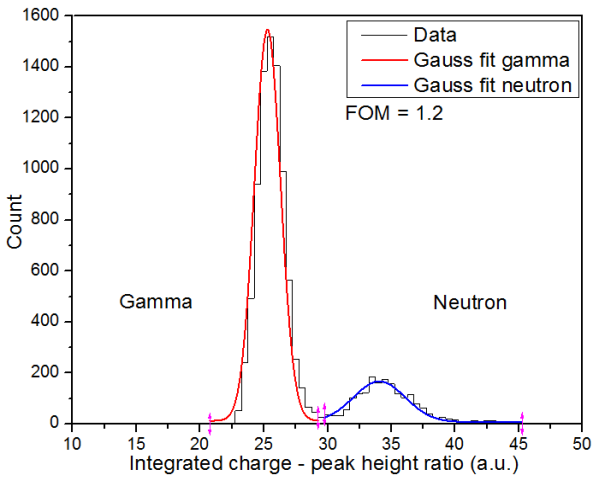


**Fig. 11.** Histogram of charge comparison

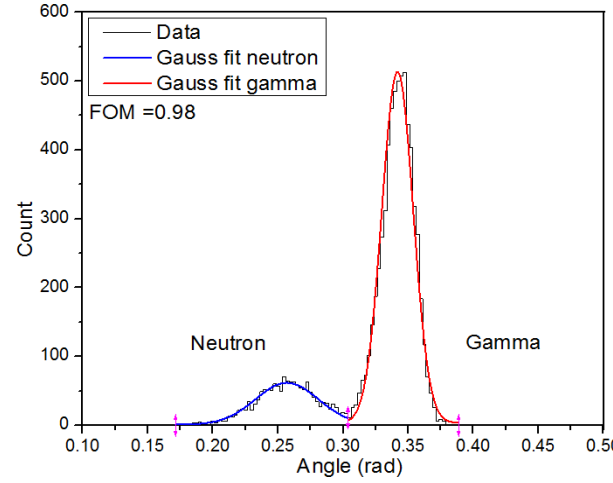


**Fig. 12.** Histogram of correlation pattern

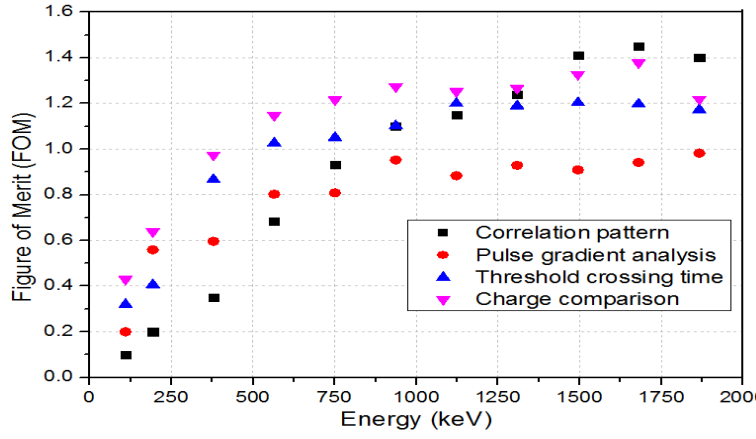


**Fig. 13.**The FOM values as a function of energy threshold corresponding with four methods as threshold crossing time, pulse gradient analysis, charge comparison, and correlation pattern recognition in the range of energy from 100keV to 2000keV

Table I shows FOM values at 700 keV energy threshold and duty time for data processing. The values in the table can be considered as specialist of the four surveyed methods.

**Table I.** The FOM values and processing time of PSD methods

| Method | FOM (at 700keV) | Processing time (ns) |
|---|---|---|
| Threshold crossing time | 1.10 | 260 ± 6 |
| Pulse gradient analysis | 0.78 | 86±2 |
| Charge comparison | 1.20 | 170 ± 3 |
| Correlation pattern recognition | 0.98 | 228 ± 2 |

### B. Discussion

The obtained FOM values were in the average range from 0.2 to 1.4. This result is suitable for the simulation estimation because the active volume of the detector was small-typed. In this detector, the FOM of CCM method was the highest in the energy region of 100 keV to 2000 keV.

The difference of FOMs between CCM and TCT is less than twenty percent, but the processing time of TCT is about thirteen percent larger than that of CCM. However the algorithm implementation for TCT method is rather simple and can easily be done on the neutron measuring system using an FPGA. The PGA method has the shortest processing time, but its' FOM is small and not stable in the surveyed energy region with the detector's small active volume.

## IV. CONCLUSIONS

This study surveyed the efficiency of distinguishing between neutron and gamma pulses from the small active volume scintillation detector using the EJ-301 liquid scintillation. The four neutron-gamma PSD algorithms were used to do the analysis and the results show that the FOM of CCM method is better than of the TCT, PGA, and CPR methods. These results are the basis for building the neutron detection systems using the EJ-301 liquid scintillation detectors with a small active volume in combination with DSP and FPGA techniques.

## REFERENCE

[1] M. L. Roush, M. A. Wilson, and W. F. Hornyak, "Pulse shape discrimination," *Nucl. Instruments Methods*, Vol. 31, No. 1, pp. 112–124, 1964.

[2] E. Bayat, N. Divani-Vais, M. M. Firoozabadi, and N. Ghal-Eh, "A comparative study on neutron-gamma discrimination with NE213 and UGLLT scintillators using zero-crossing method," *Radiat. Phys. Chem.*, Vol. 81, No. 3, pp. 217–220, 2012.

[3] J. Cerny, Z. Dolezal, M. P. Ivanov, E. S. Kuzmin, J. Svejda, and I. Wilhelm, "Study of neutron response and n--γ discrimination by charge comparison method for small liquid scintillation detector," *Nucl. Instruments Methods Phys. Res. Sect. A Accel. Spectrometers, Detect. Assoc. Equip.*, Vol. 527, No. 3, pp. 512–518, 2004.

[4] G. Liu, M. J. Joyce, X. Ma, and M. D. Aspinall, "A digital method for the discrimination of neutrons and rays with organic scintillation detectors using frequency gradient analysis," *Nucl. Sci. IEEE Trans.*, Vol. 57, No. 3, pp. 1682–1691, 2010.

[5] D. Takaku, T. Oishi, and M. Baba, "Development of neutron-gamma discrimination technique using pattern-recognition method with digital signal processing," *Prog. Nucl. Sci. Technol.*, Vol. 1, pp. 210–213, 2011.

[6] S. Marrone, D. Cano-Ott, N. Colonna, C. Domingo, F. Gramegna, E. M. Gonzalez, F. Gunsing, M. Heil, F. Käppeler, P. F. Mastinu, and others, "Pulse shape analysis of liquid scintillators for neutron studies," *Nucl. Instruments Methods Phys. Res. Sect. A Accel. Spectrometers, Detect. Assoc. Equip.*, Vol. 490, No. 1, pp. 299–307, 2002.

[7] S. D. Jastaniah and P. J. Sellin, "Digital pulse-shape algorithms for scintillation-based neutron detectors," *IEEE Trans. Nucl. Sci.*, Vol. 49 I, no. 4, pp. 1824–1828, 2002.

[8] G. F. Knoll, *Radiation Detection and Measurement*, Vol. 3. 2010.

[9] H. Spieler, "Pulse processing and analysis," *IEEE NPSS Short Course, 1993 Nucl. Sci. Symp. San Fr. Calif.*, 2002.

[10] S. Barra, S. Kouda, A. Dendouga, and N.E. Bouguechal, "Simulink behavioral modeling of a 10-bit pipelined ADC," *Int. J. Autom. Comput.*, Vol. 10, No. 2, pp. 134–142, 2013.

[11] B. D. Mellow, M. D. Aspinall, R. O. Mackin, M. J. Joyce, and A. J. Peyton, "Digital discrimination of neutrons and γ-rays in liquid scintillators using pulse gradient analysis," *Nucl. Instruments Methods Phys. Res. Sect. A Accel. Spectrometers, Detect. Assoc. Equip.*, Vol. 578, No. 1, pp. 191–197, 2007.